# Direct photolysis of benzoylecgonine under UV irradiation at 254 nm in a continuous flow **microcapillary array photoreactor**

Danilo Russo[a], Danilo Spasiano[a], Marianna Vaccaro[a], Roberto Andreozzi[a], Gianluca Li Puma[b], Nuno M Reis[b*], Raffaele Marotta[a*]

[a] Dipartimento di Ingegneria Chimica, dei Materiali e della Produzione Industriale, Università di Napoli "Federico II", p.le V. Tecchio, 80 – 80125 – Napoli, Italy.

[b] Environmental Nanocatalysis & Photoreaction Engineering Department of Chemical Engineering, Loughborough University, Loughborough LE11 3TU, UK.

**Abstract**

**Benzoylecgonine (BE) is the major metabolite of cocaine and a contaminant of emerging concern often detected in sewage treatment plant (STP) effluents and surface waters. In this study, an innovative microcapillary film (MCF) array photoreactor made of fluoropolymer material was used to determine the direct photolysis quantum yield at 254 nm of benzoylecgonine. The photolysis quantum yield of BE was found to be $(6.22 \pm 0.19) \cdot 10^{-3}$ mol· ein$^{-1}$. The proposed methodology was validated by estimating the quantum yield of caffeine $(7.48 \cdot 10^{-4} \pm 0.64) \cdot 10^{-4}$ mol·ein$^{-1}$, which was found in agreement with results published in literature. The MCF uses a very small sample volume (in the order of 330 µl per meter length of material) and allows extremely rapid photolysis with a short contact time ranging from a fraction of seconds to few minutes. The novel microfluidic-based approach presented in this study is particularly useful for determining the photochemical behavior of highly priced pharmaceuticals, illicit drugs, metabolites and uncommon or regulated substances.**

*Keywords*: **microcapillary film**, photoreactor, direct photolysis, caffeine, benzoylecgonine, cocaine metabolite, water reuse.

* *Corresponding author 1*. Tel.: +39 081 7682968; fax: +39 081 5936936. E-mail address: rmarotta@unina.it (R. Marotta).

* *Corresponding author 2*. Tel.: +44 (0)1509 2225058; fax: +44 (0)1509 223923. E-mail address: n.m.reis@lboro.ac.uk (N. M. Reis).

## 1. Introduction

**Miniaturized** reactors have attracted **significant** interest in the last decade **due to fast development** and application of **microfluidics devices** [1,2]. Microchannel reactors are very **promising of producing niche** or high-added-value fine organic chemicals [3] such as polymers [4], novel pharmaceuticals [5], peptides and biomolecules [6,7] or for carrying highly exothermic reactions [8]. **The advantages associated with the use of microreacto**rs in comparison to conventional scale reactor systems, **are shorter** reaction times, high yield and selectivity, **reduced consumption of reagents and** solvents, highly controlled process conditions, high surface-area-to-volume ratios, extremely efficient heat transfer and mass transport, reduced material costs and increased safety [9–11]. **In addition,** flow **microreactors can** be directly interfaced with several analytical **methods** such as UV/Vis spectroscopy [12], mass spectrometry [13] and chromatography [14]. **Microreactors** are also suitable for carrying out photochemical processes, as evidenced by some extended reviews, which collect recent advances in the homogeneous and heterogeneous photochemical transformations for synthetic **purposes**, thus **highlighting the potential** of miniaturized photoreactors **as cleaner and efficient chemical production platforms** [15–17]. **In order to optimize the design and operation** of miniaturized photoreactors for chemical process intensificatio**n,** and to **develop** suitable kinetic models able to predict **the performance** of these system**s, it is crucial to investigate the** fluid-**dynamics, the radiation field and other crucial**

2

**operational factors of continuous-flow** photoreactors. Currently, only few papers have **studied** the effect **of these parameters on the** efficiency of micro-photoreactors [18-19].

In the present **study**, **a** novel fluoropolymer microcapillary film (MCF) photoreactor recently presented [20] **was used to investigate** the photolytic degradation of benzoylecgonine (BE), a major human metabolite of cocaine, whose presence has been often documented in Sewage Treatment Plant (STP) effluents and surface water at concentrations of $0.1 - 3275$ ng·L$^{-1}$ [21–22] and of $0.3 - 520$ ng·L$^{-1}$ [23–25] respectively. **BE is so diffused in European surface and ground waters that its monitoring has** been proposed as a statistical indicator for estimating the number of cocaine users in each region [26,27]. It is particularly **relevant** to **study** the **photodegradation of** this emerging environmental **contaminant** under UV$_{254}$ irradiation as **UV is rapidly being adopted for polishing STP** effluents and **for water reuse in** irrigation or public works [28,29]. Although concentrations **of BE in** sewage and surface water**s** are normally low, a potential negative impact of the presence of BE and its parent compounds (i.e. ecgonine) **towards** living organisms cannot be ruled out [30–32], particularly for water **reused in agriculture**.

**MCF microreactor technology, in this study made of 10 multiple parallel microcapillaries with a small 200 μm internal diameter, is ideal for studying the photolysis at UV$_{254}$ of BE and other contaminants in water due to several advantages including [20]: (i) very high UV optical transparency of the material of construction (>90% according to the manufacturer of Teflon-FEP resin, Dupont); (ii) the irradiation of the solution with straight rays and uniform photon flux and (iii) small sample volumes which is particularly needed with controlled substances such as BE. The manufacturing of the MCF with Teflon-FEP (a material with a similar refractive index as that of water) allowed the construction of the MCF as a continuous plastic film containing a parallel array of microcapillaries with controlled size and shape** [33]. This study is one of the few examples in literature which uses a micro-photoreactor **to investigate the photodegradation kinetics** of a contaminant of emerging concern.

## 2. Materials and Methods

### 2.1. Materials

The MCF was produced by Lamina Dielectrics Ltd (Billingshurst, West Sussex, UK) from Teflon® FEP (Dupont, USA) using a novel melt-extrusion process [34]. Blue Dextran 70 (TdB Consultancy AB, Sweden) dissolved in water (1000 ppm) was used as a tracer for determining the residence time distribution (RTD) in the MCF. Hydrogen peroxide (30% v/v), benzoylecgonine (BE, ≥ 99.0% w/w), caffeine (CAF, 99% w/w), methanol (≥99.9% v/v), acetonitrile (≥99.9% v/v), and formic acid (≥95% v/v) were sourced from Sigma-Aldrich (UK). All reagents were used as received and milli-Q water was used as solvent in analytical determinations and experiments.

### 2.2. Experimental apparatus and procedures

The MCF consisted of a 5 mm wide fluoropolymer film with flat surfaces containing an array of 10 parallel capillaries embedded in the film with length ($L$) of 2.2 m and mean hydraulic diameter ($d$) of 195 μm (Fig. 1). The diameter of the microcapillaries was determined optically using an optical trinocular stereo zoom microscope equipped with a digital camera (Nikon SMZ 1500). Prior to analysis the MCF samples were immersed in liquid nitrogen to reduce the elastic behavior of the film and avoid deformation of the material during the slicing with a fresh razor blade.

The liquid was pumped through the MCF using a M Series syringe-free liquid handling pump (Valco Instruments Co. Inc. VICI AG International) capable of operating in the flow range of 5 nL·min$^{-1}$ to 10 mL·min$^{-1}$. The RTD experiments required two pumps to flow the water and the tracer aqueous solution.

The array photoreactor consisted of the MCF coiled around a tubular germicidal lamp (Germicidal G8T5, GE Lighting, Northampton, UK) emitting radiation at 254 nm with a nominal power of 8 W (Fig. 2). The lamp bulb was 302 mm long and with a diameter of 16 mm. The film was held in place by two plastic pegs in the center section of the lamp in which light irradiance was found

uniform. **The section** of the MCF not **coiled around the germicidal lamp was** covered with aluminum foil **to prevent light irradiation. The residence time in the reactor and exposure to UV was varied by varying the length of MCF coiled over the lamp**.

**The lamp irradiance and therefore the incident flux in the capillaries** was varied by changing the nominal power supplied to the lamp from 4.5 W to 8.**0** W using a variable power supply unit. The reactor was operated in **continuous mode** until steady state was reached ($\cong$ 200 s, **i.e. 3 to 5 times the mean hydraulic time**). Samples were **then collected at both outlet and** inlet of the MCF **photoreactor and** rapidly analyzed. **To** avoid operation **at excessive** pressure drop**s**, the solution was recirculated to achieve reaction times higher than the mean **residence time in the** MCF.

All the experimental runs were carried out at room temperature (20 °C), **and the temperature of the fluids remained constant along the experiment (data not shown). The** pH of **the solutions** was **adjusted using diluted** solutions of NaOH and $H_2SO_4$. At the end of each experimental run, the pH of the solutions was **unchanged**.

**For RTD determination two** pumps connected to **an automatic multi-inlet** valve **was used to switch** the inlet of the MCF from **clean** water to the Blue Dextran **solution. Each experiment started by following water through the microreactor until a baseline was established in the UV detector (see section 2.3). The valve was then switched to the** tracer **solution producing a step change in concentration**, and monitored until **the outlet** reached **a st**ationary state (i.e., three to five times the mean residence time).

### 2.3. Analytical methods

**The** entire section of the MCF material was imaged real-time in UV for measuring the RTD tracer **using** an ActiPix™ D100 UV Area Imaging System microfluidic monitor (Paraytec, York, UK) equipped with a 214 nm dichronic filter. **The viscosity of the tracer solution was determined using a** AR1000-N (TA Instruments) **rotational** rheomet**er**.

The concentrations of hydrogen peroxide, BE and **caffeine in the samples** were evaluated by HPLC (1100 Agilent) equipped with a Gemini C18 (Phenomenex) reverse phase column and a diode array UV/VIS detector ($\lambda = 232$ and 274 nm) and using a mobile phase flowing at 0.8 mL·min$^{-1}$. The mobile phase **used for** hydrogen peroxide and BE analyses **consisted of a** mixture of formic acid aqueous solution (25 mM) (A) and acetonitrile (B). The gradient **used** was as follow**s:** 7% B to 28% B for 9 min, increased to 50% B in 5 min, constant for 2 min, and then decreased to 35.7% B in 3 min and, finally to 7% B in 5 min. The mobile phase for caffeine analysis **consisted of formic** acid aqueous solution (25 mM) (A) and methanol (C). In this case a linear gradient progressed from 5% C to 80% C in 14 min and then decreased to the initial conditions **after 5** min. The initial and final pH of **the solutions was** measured with an Accumet Basic AB10 pH-meter. The molar **absorption** coefficients of caffeine and benzoylecgonine were estimated using a Perkin Elmer UV/VIS spectrometer (mod. Lambda 35).

## 3. Results and discussion

### 3.1. RTD determination

**Rheological measurements were performed to determine the viscosity of the RTD tracer as a function of the shear rate. Figure 3 shows that the tracer solution viscosity remained very close to that of water and that was unaffected by shear rate. Varying the shear rate in the range 2-1000 s$^{-1}$, the ratio between the tracer and water viscosities remained close to 1.0.**

The dynamic response of the **normalized cumulative** tracer concentration (empty circles) at the output of the MCF reactor for a step change at two different flow rates (0.6 mL·min$^{-1}$ and 1.0 mL·min$^{-1}$) is shown in Figures 4a–b respectively. The **theoretical curve** for an ideal Plug Flow Reactor (PFR, continuous line) and **pure convective or** Laminar Flow Reactor (LFR, dashed lines) are also shown.

Although the Reynolds number **was well within the laminar flow regime** (6.5 and 10.9 for flow rates of 0.6 mL·min$^{-1}$ and 1.0 mL·min$^{-1}$ respectively) **the hydrodynamic** behavior **in** the reactor approached that of an **axially dispersed PFR**, rather than a LFR. Similar **observations** have been reported in **other studies in microreactors** [35-38] and it was in agreement **with Taylor's** theory **on** axial dispersion in reactors with a small $d/L$ ratio [39].

The MCF experimental **data fitted well a** Gaussian cumulative distribution function (CDF). The mean value **and variance** of the **CDF** distribution **fitted well both** the mean residence time and the axial dispersion in the **reactor. The mean hydraulic time** (39.7 s for 1.0 mL·min$^{-1}$ and 66.2 s for 0.6 mL·min$^{-1}$) **matched closely** the mean residence time determined **from the** experimental RTD data (40.5 s and 65.4 s, respectively), which **also revealed the absence of dead volumes or sorption of the tracer on the microcapillaries walls** [40].

The extent of axial dispersion in the MCF was estimated **by fitting RTD data to a PFR with axial dispersion model, by finding the dimensionless** dispersion number ($N_D$), **which is given by** the ratio of the axial **dispersion ($D$)** and the product of superficial velocity ($u$) and the reactor length ($L$):

$$N_D = \frac{D}{u \cdot L} \tag{1}$$

Depending on **the magnitude of axial** dispersion, **one of** the two following **PFR with axial dispersion models was used** [40]:

$$E = \sqrt{\frac{u^3}{4\pi DL}} \cdot exp\left[-\frac{(L-ut)^2}{\frac{4DL}{u}}\right] \qquad \text{(for } N_D < 0.01) \tag{2}$$

$$\left(\frac{\sigma}{\tau}\right)^2 = 2N_D - 2N_D^2 \cdot (1 - e^{-\frac{1}{N_D}}) \quad \textbf{(for } N_D > 0.01) \tag{3}$$

where $E$ and $\sigma$ represent the residence time distribution and the standard deviation respectively. Equation 2 can be easily reported as a function of $N_D$ and the ideal residence time $\tau$:

$$E = \sqrt{\frac{u^2}{4\pi L^2 N_D}} \cdot exp\left[-\frac{(L-ut)^2}{4L^2 N_D}\right] = \frac{1}{\tau}\sqrt{\frac{1}{4\pi N_D}} \cdot exp\left[-\frac{(t-\tau)^2}{4\tau^2 N_D}\right] \tag{4}$$

The $N_D$ values estimated from Equations 3 and 4 for the two flow rate conditions yielded very similar results (Table 1). Levenspiel reports that a tubular reactor can be successfully modeled as a PFR when $N_D$ is lower than 0.01 **[40], however, other** studies have shown that even for $N_D < 0.05$, the PFR model **yields very** reliable results in term of conversion [38]. **Therefore, the MCF photoreactor was considered an ideal PFR in the photolysis experiments.**

### 3.2. Optical path length

Due to the absence of refractive phenomena [20], it can be assumed that the radiation emitted by the UV lamp is perpendicular to the surface of the bulb and crosses both the reactor and the reacting solution without any deviation **of path length. Considering** the circular section of the capillaries, the optical path length **is determined by the in**tersection between the single UV ray and the capillary section.

As shown in Figure **5, there** is only one ray **on each capillary** that crosses the section along **the diameter** length (chord $c$-$c'$). On the other hand, most of the UV rays cross the capillaries along a path shorter than the diameter (e.g. chords $a$-$a'$ and $b$-$b'$). **In consequence**, the average diameter of the capillaries could not be taken as the average optical path length in the MCF. In contrast, the optical path length ($l$) of the capillaries was calculated as ratio between the mean hydraulic section ($S$) and the mean diameter of the capillaries ($d$) as **follows**:

$$l = \frac{S}{d} = \frac{\pi \cdot d^2}{4 \cdot d} = 152 \ \mu m \tag{5}$$

This operation corresponds to the mean integral value of the chords parallel to the incident radiation. Therefore, the cross section of a single capillary was considered to be equivalent to a rectangle **(indicated in Figure 5 as equivalent section)** oriented as shown in Figure 5 and with the same cross sectional area ($S$) **as that** of the circular capillary **(indicated in Figure 5 as real section)**.

8

### 3.3. Estimation of lamp $UV_{254}$ photon flux

In order to better characterize the micro-photoreactor, the $UV_{254}$ photon flux ($q_{p,254}$) [41] incident on the reactor was first estimated. For microchannel reactors, this parameter **is difficult to be directly estimated through radiometric measurements because of errors originating from measuring the flux from very small reactor surfaces and possible reflection phenomena from the surrounds. Therefore, the photon flux was estimated from an indirect approach by determining the photolysis of an aqueous solution of hydrogen peroxide (reactions $r_1$ - $r_3$) at 254 nm [42] which was flowed through MCF.**

$$H_2O_2 \xrightarrow{h\nu,\ \Phi_{254}^{H_2O_2}} 2\ HO° \qquad\qquad \Phi_{254}^{H_2O_2} = \textbf{0.55}\ \text{mol·}\textbf{ein}^{-1} \quad [43] \qquad\qquad (r_1)$$

$$HO° +\ H_2O_2 \xrightarrow{k_h} HO_2° + H_2O \qquad\qquad k_h = 2.7{\cdot}10^7\ \text{L·mol}^{-1}{\cdot}\text{s}^{-1}\ [44] \qquad\qquad (r_2)$$

$$HO_2° + HO_2° \xrightarrow{k_t} H_2O_2 + O_2 \qquad\qquad k_t = 8.3{\cdot}10^5\ \text{L·mol}^{-1}{\cdot}\text{s}^{-1}\ [45] \qquad\qquad (r_3)$$

**Considering the radical species** ($HO_2°$ and $HO°$) **at steady-state, the mass balance on** hydrogen peroxide **yielded**:

$$\frac{d[H_2O_2]}{d\tau} = -2\frac{q_{p,254}}{V} \cdot \Phi_{254}^{H_2O_2} \cdot \left(1 - \exp\left(-2.3 \cdot l \cdot \varepsilon_{254}^{H_2O_2} \cdot [H_2O_2]\right)\right) \qquad\qquad (6)$$

where "$l$" is the optical pathlength of the micro-photoreactor, previously calculated (152 μm), "$\varepsilon_{254}^{H_2O_2}$" the molar **absorption** coefficient at 254 nm for hydrogen peroxide (18.6 L·mol$^{-1}$·cm$^{-1}$), $V$ the volume of reacting system (0.45 mL), "$\Phi_{254}^{H_2O_2}$" the primary quantum yield of the direct photolysis of hydrogen peroxide at 254 nm and $\tau$ the **residence** time. The photon flux "$q_{p,254}$" was estimated by **an iterative method**, which minimized the objective function $\sum_{i=1}^{n}(y_i - c_i)^2$, i.e., the squares of the differences between the calculated "$y$" and experimental "$c$"

9

concentrations of hydrogen peroxide [46], where "$n$" is the number of experimental data collected during the photolysis of $H_2O_2$.

**The ordinary differential equation (Eq. 6) was solved using MATLAB routine "ode45", which is based on the Runge-Kutta method with adaptive step-size**. The numerical values for the $UV_{254}$ incident photon fluxes for two nominal lamp powers ($P_N$) **and their** uncertainties and percentage standard deviations ($\sigma_\%$) are reported in Table 2.

The **photolysis of hydrogen peroxide determined experimentally was compared to the values predicted by** the kinetic **model, and this showed a goof fit (Figure 6).**

In order to compare the nominal UV power ($P_N$) and the effective one, the latter has been expressed in watts ($P_{254}^o$) using the following **equation**:

$$P_{254}^o = \frac{q_{p,254} \cdot h \cdot N_a \cdot c}{\lambda} \tag{7}$$

where "$h$" is Planck's constant ($6.63 \cdot 10^{-34}$ J·s), "$c$" the speed of light in vacuum ($3.0 \cdot 10^8$ m·s$^{-1}$), "$N_a$" **Avogadro's constant** ($6.02 \cdot 10^{23}$) and "$\lambda$" the wavelength of the radiation emitted by the UV lamp ($254 \cdot 10^{-9}$ m).

### 3.3. Model validation

The **accuracy of the** modeling methodology for the MCF **was validated by estimating the quantum yield of direct photolysis of caffeine at** 254 nm ($\Phi_{254}^{CAF}$) in the MCF and **determining its difference from the quantum yield values reported in literature**. Caffeine is often used as reference compound since it is considered an anthropogenic marker of wastewater contamination in surface waters [47]. **The quantum yield of caffeine, shown in Table 3, was calculated using the same** optimization procedure previously reported for the estimation **of** "$q_{p,254}$":

$$\frac{d[CAF]}{dt} = -\frac{q_{p,254}}{V} \cdot \Phi_{254}^{CAF} \cdot (1 - \exp(-2.3 \cdot l \cdot \varepsilon_{254}^{CAF} \cdot [CAF])) \tag{8}$$

where the term "$\varepsilon_{254}^{CAF}$" is the molar **absorption** coefficient at 254 nm for caffeine (4175 L·mol$^{-1}$·cm$^{-1}$). **Literature data obtained using different photoreactor designs are also reported.** Figure 7 shows the UV$_{254}$ photodegradation of caffeine in the MCF as a function of the **irradiation** time and the model prediction (equation 8) using the quantum yield values reported in Table 3. The model was able to predict the photodegradation of caffeine with a **good** degree of confidence. The experimental results (full circles) **were within the results of determined from equation 8 using the quantum yields from other** studies (dashed line).

### 3.4. Direct photolysis of benzoylecgonine

**The direct photolysis of BE under UV$_{254}$ irradiation was determined using the MCF photoreactor.** Figure 8 shows that the **rate** of BE photolysis **was** not affected **by pH** in the range from pH 4.0 to 8.0. **A**dditional **control** runs, carried out at pH 4.0, under dark conditions or with UV$_{254}$ irradiation but under an inert atmosphere (**n**itrogen bubbling), **showed no** difference in the photolysis of BE with respect to the data reported in Figure 8 (data not shown). This rules out the occurrence of hydrolytic mechanisms or photooxidative processes due to the presence of oxidant species such hydroxyl radicals or singlet oxygen than may be eventually produced under aerated conditions [50].

Following the same methodology reported for caffeine, the quantum yield of direct photolysis of BE ($\Phi_{254}^{BE}$) was estimated using simultaneously the data collected from two photolytic runs carried at pH 4.0 and 8.0 under irradiation with the UV$_{254}$ lamp with a nominal power of 8.**0** W (*optimization mode*). Moreover, with the aim to validate the best estimate of $\Phi_{254}^{BE}$, the results of an additional photolytic run, carried out at pH 6.0 with the UV$_{254}$ lamp with a nominal power of 4.5 W, were modeled without any further adjustment of the $\Phi_{254}^{BE}$ parameter (*fitting mode*).

Table 4 shows the quantum yield for direct photolysis of BE $\Phi_{254}^{BE}$, the uncertainty percentage and standard deviations calculated on each experimental run.

The graphical comparison of the predicted and measured BE concentrations during the photolytic process is reported in Figure 9 for the set used in *optimization mode* and in Figure 10 for the data used in *fitting mode*. The analysis of the figures suggest a high degree of confidence of the proposed model to predict the photolytic decomposition of BE under the adopted experimental conditions.

## 4. Conclusions

A **MCF** array photoreactor made of fluoropolymer material was characterized by measuring the RTD. The flow regime was found to be approximately in the plug flow region at mean flow velocities below 1 mL·min$^{-1}$. The data of a first set of experimental runs **on the MCF** was used to predict the quantum yield of direct photolysis at 254 nm of caffeine (**(7.48±0.64)·10$^{-4}$** mol·**ein**$^{-1}$) in unbuffered aqueous solutions.

The estimated value was located within the variability range previously identified by others through the results of measurements carried out in different conventional reactors.

Direct photolysis at 254 nm of benzoylecgonine was investigated in the pH range of 4.0 – 8.0. The consumption rates were not affected by the pH adopted. **The photolysis** quantum yield **was (6.22±0.19)·10$^{-3}$** mol·**ein**$^{-1}$.

The results collected demonstrate that the MCF photoreactor, adopted in the present investigation, is particularly useful for investigating the photochemical behavior of highly priced pharmaceuticals and illicit drugs and their human metabolites.

**References**

[1] W.Y Lin, Y. Wang, S. Wang, H.R. Tseng. Integrated microfluidic reactors. Nano Today 4 (2009) 470–481.

[2] P.L.Mills, D.J. Quiram, J.F. Ryley. Microreactor technology and process miniaturization for catalytic reactions–A perspective on recent developments and emerging technologies. Chem Eng. Sci. 62 (2007) 6992–7010.

[3] T. Wirth. Microreactors in Organic Chemistry and Catalysis, Ed. Wiley-VCH Verlag GmbH & Co. KGaA, Germany, 2013.

[4] Z. Nie, S. Xu, M. Seo, P.C. Lewis, E. Kumacheva. Polymer particles with various shapes and morphologies produced in continuous microfluidic reactors. J. Am. Chem. Soc. 127 (2005) 8058–8063.

[5] D.M. Roberge, L. Ducry, N. Bieler, P. Cretton, B. Zimmermann. Microreactor technology: A revolution for the fine chemical and pharmaceutical industries? Chem. Eng. Technol. 28 (2005) 318–323.

[6] F.R. Carrel, K. Geyer, J.D.C. Codee, P.H. Seeberger. Oligosaccharide synthesis in microreactors. Org. Lett. 9 (2007) 2285–2288.

[7] K. Geyer, P.H. Seeberger. Optimization of glycosylation reactions in a microreactor. Helv. Chim. Acta 90 (2007) 395–403.

[8] J. Pelleter, F. Renaud. Facile, fast and safe process development of nitration and bromination reactions using continuous flow reactors. Org. Process Res. Dev. 13 (2009) 698–705.

[9] H. Löwe, V. Hessel, A. Mueller. Microreactors. Prospects already achieved and possible misuse. Pure Appl. Chem. 74(12) (2002) 2271–2276.

[10] X. Zhang, S. Stefanick, F.J. Villani. Application of microreactor technology in process development. Org. Process Res. Dev 8 (2004) 455–460.

[11] B.P. Mason, K.E. Price, J.L. Steinbacher, A.R. Bogdan, D.T. McQuade. Greener approaches to organic synthesis using microreactor technology. Chem. Rev. 107 (2007) 2300–2318.

[12] E.M. Chan, A.P. Alivisatos, R.A. Mathies. High-temperature microfluidic synthesis of CdSe nanocrystals in nanoliter droplets. J. Am. Chem. Soc. 127(40) (2005) 13854–13861.

[13] R.M. Schoenherr, M.L. Ye, M. Vannatta, N.J. Dovichi, CE-microreactor-CE-MS/MS for protein analysis. Anal. Chem. 79 (2007) 2230–2238.

[14] R.A. Brennen, H. Yin, K.P. Killeen, Microfluidic gradient formation for nanoflow chip, Anal. Chem. 79(24) (2007) 9302–9309.

[15] M. Oelgemöller, O. Shvydkiv, Recent advances in microflow photochemistry. Molecules 16 (2011) 7522–7550.

[16] M. Oelgemöller, Highlights of photochemical reactions in microflow reactors, Chem. Eng. Technol. 35(7) (2012) 1144–1152.

[17] E.E. Coyle, M. Oelgemöller. Micro-photochemistry: photochemistry in microstructured reactors. The new photochemistry of the future? Photochem. Photobiol. Sci. 7 (2008) 1313–1322.

[18] S. Hejda, M. Drhova, J. Kristal, D. Buzek, P. Krystynik, P. Kluson, Microreactor as efficient tool for light induced oxidation reactions, Chem. Eng. J. 255 (2014) 178–184.

[19] S. Aida, K. Terao, Y. Nishiyama, K. Kakiuchi, M. Oelgemoller, Microflow photochemistry—a reactor comparison study using the photochemical synthesis of terebic acid as a model reaction, Tetrahedron Lett. 53 (2012) 5578–5581.

[20] N.M. Reis, G. Li Puma, Novel microfluidics approach for extremely fast and efficient photochemical transformations in fluoropolymer microcapillary films, Chem. Commun. **51 (2015) 8414–8417**.

[21] M. Huerta-Fontela, M.T. Galceran, J. Martin, F. Ventura, Occurrence of psychoactive stimulatory drugs in wastewaters in north-eastern Spain, Sci. Total Environ. 397 (2008) 31–40.

[22] B. Kasprzyk-Hordern, R.M. Dinsdale, A.J. Guwy, The removal of pharmaceuticals, personal care products, endocrine disruptors and illicit drugs during wastewater treatment and its impact on the quality of receiving waters. Water Res. 43 (2009) 363–380.

[23] J.D. Berset, R. Brenneisen, C. Mathieu, Analysis of llicit and illicit drugs in waste, surface and lake water samples using large volume direct injection high performance liquid chromatography – Electrospray tandem mass spectrometry (HPLC–MS/MS), Chemosphere. 81 (2010) 859–866.

[24] A.L.N. Van Nuijs, B. Pecceu, L. Theunis, N. Dubois, C. Charlier, P.G. Jorens, L. Bervoets, R. Blust, H. Neels, A. Covaci. Cocaine and metabolites in waste and surface water across Belgium. Environ. Pollut. 157 (2009)123–129.

[25] E. Zuccato, S. Castiglioni, R. Bagnati, C. Chiabrando, P. Grassi, R. Fanelli, Illicit drugs, a novel group of environmental contaminants. Water Res. 42 (2008a) 961–968.

[26] E. Zuccato, C. Chiabrando, S. Castiglioni, R. Bagnati, R. Fanelli, Estimating community drug abuse by wastewater analysis. Environ. Health Perspect. 116 (2008b) 1027–1032.

[27] A.L.N. van Nuijs, S. Castiglioni, I. Tarcomnicu, C. Postigo, M.J. Lopez de Alda, H. Neels, E. Zuccato, D. Barcelo, A. Covaci, Illicit drug consumption estimations derived from wastewater analysis: a critical review, Sci. Total Environ. 409 (2011) 3564–3577.

[28] G. Orona, C. Campos, L. Gillerman, M. Salgot, Wastewater treatment, renovation and reuse for agricultural irrigation in small communities, Agr. Water Manage. 38(3) (1999) 223–234.

[29] D. Christova-Boal, R.E. Eden, S. McFarlane. An investigation into greywater reuse for urban residential properties. Desalination. 106(1–3) (1996) 391–397.

[30] A. Binelli, I. Marisa, M. Fedorova, R. Hoffmann, C. Riva, First evidence of protein profile alteration due to the main cocaine metabolite (benzoylecgonine) in a freshwater biological model, Aquat. Toxicol. 140–141 (2013) 268–278.

[31] M. Parolini, A. Binelli, Adverse effects induced by ecgonine methyl ester to the zebra mussel: A comparison with the benzoylecgonine, Environ. Pollut. 182 (2013b) 371–378.

[32] M. Parolini, A. Pedriali, C. Riva, A. Binelli, Sub-lethal effects caused by the cocaine metabolite benzoylecgonine to the freshwater mussel *Dreissena polymorpha*, Sci. Total Environ. 444 (2013a) 43–50.

[33] A.I. Barbosa, A.P. Castanheira, A.D. Edwards, N.M. Reis, A lab-in-a-briefcase for rapid prostate specific antigen (PSA) screening from whole blood,. Lab Chip. 14 (2014) 2918–2928.

[34] B. Hallmark, F. Gadala-Maria, M.R. Mackley, The melt processing of polymer microcapillary film (MCF), J. Non-Newtonian Fluid Mech. 128 (2005) 83–98.

[35] F. Trachsel, A. Günther, S. Khan, K.F. Jensen, Measurement of residence time distribution in microfluidic systems, Chem. Eng. Sci. 60 (2005) 5729–5737.

[36] C.H. Hornung, M.R. Mackley, The measurement and chatacterisation of residence time distributions for laminar liquid flow in plastic microcapillary arrays, Chem. Eng. Sci. 64 (2009) 3889–3902.

[37] C.H. Hornung, B. Hallmark, M. Baumann, I.R. Baxendale, S.V. Ley, P. Hester, P. Clayton, M.R. Mackley, Ind. Eng. Chem. Res. 49 (2010) 4576–4582.

[38] E. Georget, J.L. Sauvageat, A. Burbidge, A. Mathys, Residence time distributions in a modular micro reaction system, J. Food Eng. 116 (2013) 910-919.

[39] G. Taylor, Dispersion of soluble matter in solvent flowing slowly through a tube, Proc. R. Soc. A. 219 (1953) 186.

[40] O. Levenspiel, Chemical Reaction Engineering, third ed., John Wiley & Sons, New York, 1999.

[41] IUPAC. Compendium of Chemical Terminology, 2nd ed. (the "Gold Book"). Compiled by A. D. McNaught and A. Wilkinson. Blackwell Scientific Publications, Oxford (1997).

[42] I. Nicole, J. De Laat, M. Doré, J.P. Duguet, C. Bonnel, Use of UV radiation in water treatment: measurement of photonic flux by hydrogen peroxide actinometry, Water Res. 24 (1990) 157-168.

[43] S. Goldstein, D. Aschengrau, Y. Diamant, J. Rabani, Photolysis of aqueous $H_2O_2$: quantum yield and applications for polychromatic UV actinometry in photoreactors, Environ. Sci. Technol. 41 (2007) 7486–7490.

[44] G.V. Buxton, C.L. Greenstock, W.P. Helman, A.B. Ross, Critical review of rate constants for reactions of hydrated electrons, hydrogen atoms and hydroxyl radicals (OH/O$^-$) in aqueous solution, J. Phys. Chem. Ref. Data 17 (1988) 513–886.

[45] B.H. Bielski, D.E. Cabelli, R.L. Aruda, A.B. Ross, Reactivity of $HO_2/O_2$ radicals in aqueous solution, J. Phys. Chem. Ref. Data 14 (1985) 1041–1077.

[46] G.V. Reklaitis, A. Ravindran, K.M. Regsdell, Engineering Optimization, Wiley, New York, 1983.

[47] I.J. Buerge, T. Poigner, M.D. Müller, H.R. Buser. Caffeine, an anthropogenic marker for wastewater contamination of surface waters. Environ. Sci. Technol. 37 (2003) 691–700.

[48] Z. Shu, J. R. Bolton, M. Belosevic, M. G. El Din, Photodegradation of emerging micropollutants using the medium-pressure UV/$H_2O_2$ Advanced Oxidation Process, Water Res. 47 (2013) 2881-2889.

[49] J. Rivas, O. Gimeno, T. Borralho, J. Sagasti, UV-C and UV-C/peroxide elimination of selected pharmaceuticals in secondary effluents, Desalination. 279 (2011) 115–120.

[50] R. Marotta, D. Spasiano, I. Di Somma, R. Andreozzi. Photodegradation of naproxen and its photoproducts in aqueous solution at 254 nm: a kinetic investigation. Wat Res. 47 (2013) 373–383.

# Direct photolysis of benzoylecgonine under UV irradiation at 254 nm in a continuous flow microcapillary array photoreactor

Danilo Russo[a], Danilo Spasiano[a], Marianna Vaccaro[a], Roberto Andreozzi[a], Gianluca Li Puma[b], Nuno M Reis[b*], Raffaele Marotta[a*]


[a] Dipartimento di Ingegneria Chimica, dei Materiali e della Produzione Industriale, Università di Napoli "Federico II", p.le V. Tecchio, 80 – 80125 – Napoli, Italy.

[b] Environmental Nanocatalysis & Photoreaction Engineering Department of Chemical Engineering, Loughborough University, Loughborough LE11 3TU, UK.

Abstract

Benzoylecgonine (BE) is the major metabolite of cocaine and a contaminant of emerging concern often detected in sewage treatment plant (STP) effluents and surface waters. In this study, an innovative microcapillary film (MCF) array photoreactor made of fluoropolymer material was used to determine the direct photolysis quantum yield at 254 nm of benzoylecgonine. The photolysis quantum yield of BE was found to be $(6.22 \pm 0.19) \cdot 10^{-3}$ mol· ein$^{-1}$. The proposed methodology was validated by estimating the quantum yield of caffeine $(7.48 \cdot 10^{-4} \pm 0.64) \cdot 10^{-4}$ mol·ein$^{-1}$, which was found in agreement with results published in literature. The MCF uses a very small sample volume (in the order of 330 µl per meter length of material) and allows extremely rapid photolysis with a short contact time ranging from a fraction of seconds to few minutes. The novel microfluidic-based approach presented in this study is particularly useful for determining the photochemical behavior of highly priced pharmaceuticals, illicit drugs, metabolites and uncommon or regulated substances.

* *Corresponding author 1*. Tel.: +39 081 7682968; fax: +39 081 5936936. E-mail address: rmarotta@unina.it (R. Marotta).

* *Corresponding author 2*. Tel.: +44 (0)1509 2225058; fax: +44 (0)1509 223923. E-mail address: n.m.reis@lboro.ac.uk (N. M. Reis).

1.  Introduction

Miniaturized reactors have attracted significant interest in the last decade due to fast development and application of microfluidics devices [1,2]. Microchannel reactors are very promising of producing niche or high-added-value fine organic chemicals [3] such as polymers [4], novel pharmaceuticals [5], peptides and biomolecules [6,7] or for carrying highly exothermic reactions [8]. The advantages associated with the use of microreactors in comparison to conventional scale reactor systems, are shorter reaction times, high yield and selectivity, reduced consumption of reagents and solvents, highly controlled process conditions, high surface-area-to-volume ratios, extremely efficient heat transfer and mass transport, reduced material costs and increased safety [9–11]. In addition, flow microreactors can be directly interfaced with several analytical methods such as UV/Vis spectroscopy [12], mass spectrometry [13] and chromatography [14]. Microreactors are also suitable for carrying out photochemical processes, as evidenced by some extended reviews, which collect recent advances in the homogeneous and heterogeneous photochemical transformations for synthetic purposes, thus highlighting the potential of miniaturized photoreactors as cleaner and efficient chemical production platforms [15–17]. In order to optimize the design and operation of miniaturized photoreactors for chemical process intensification, and to develop suitable kinetic models able to predict the performance of these systems, it is crucial to investigate the fluid-dynamics, the radiation field and other crucial operational factors of continuous-flow photoreactors.

2

Currently, only few papers have studied the effect of these parameters on the efficiency of micro-photoreactors [18-19].

In the present study, a novel fluoropolymer microcapillary film (MCF) photoreactor recently presented [20] was used to investigate the photolytic degradation of benzoylecgonine (BE), a major human metabolite of cocaine, whose presence has been often documented in Sewage Treatment Plant (STP) effluents and surface water at concentrations of $0.1 - 3275$ ng$\cdot$L$^{-1}$ [21–22] and of $0.3 - 520$ ng$\cdot$L$^{-1}$ [23–25] respectively. BE is so diffused in European surface and ground waters that its monitoring has been proposed as a statistical indicator for estimating the number of cocaine users in each region [26,27]. It is particularly relevant to study the photodegradation of this emerging environmental contaminant under UV$_{254}$ irradiation as UV is rapidly being adopted for polishing STP effluents and for water reuse in irrigation or public works [28,29]. Although concentrations of BE in sewage and surface waters are normally low, a potential negative impact of the presence of BE and its parent compounds (i.e. ecgonine) towards living organisms cannot be ruled out [30–32], particularly for water reused in agriculture.

MCF microreactor technology, in this study made of 10 multiple parallel microcapillaries with a small 200 µm internal diameter, is ideal for studying the photolysis at UV$_{254}$ of BE and other contaminants in water due to several advantages including [20]: (i) very high UV optical transparency of the material of construction (>90% according to the manufacturer of Teflon-FEP resin, Dupont); (ii) the irradiation of the solution with straight rays and uniform photon flux and (iii) small sample volumes which is particularly needed with controlled substances such as BE. The manufacturing of the MCF with Teflon-FEP (a material with a similar refractive index as that of water) allowed the construction of the MCF as a continuous plastic film containing a parallel array of microcapillaries with controlled size and shape [33]. This study is one of the few examples in literature which uses a micro-photoreactor to investigate the photodegradation kinetics of a contaminant of emerging concern.

2. Materials and Methods

2.1. Materials

The MCF was produced by Lamina Dielectrics Ltd (Billingshurst, West Sussex, UK) from Teflon®

FEP (Dupont, USA) using a novel melt-extrusion process [34]. Blue Dextran 70 (TdB Consultancy

AB, Sweden) dissolved in water (1000 ppm) was used as a tracer for determining the residence time

distribution (RTD) in the MCF. Hydrogen peroxide (30% v/v), benzoylecgonine (BE, ≥ 99.0%

w/w), caffeine (CAF, 99% w/w), methanol (≥99.9% v/v), acetonitrile (≥99.9% v/v), and formic

acid (≥95% v/v) were sourced from Sigma-Aldrich (UK). All reagents were used as received and

milli-Q water was used as solvent in analytical determinations and experiments.


2.2. Experimental apparatus and procedures

The MCF consisted of a 5 mm wide fluoropolymer film with flat surfaces containing an array of 10

parallel capillaries embedded in the film with length ($L$) of 2.2 m and mean hydraulic diameter ($d$)

of 195 μm (Fig. 1). The diameter of the microcapillaries was determined optically using an optical

trinocular stereo zoom microscope equipped with a digital camera (Nikon SMZ 1500). Prior to

analysis the MCF samples were immersed in liquid nitrogen to reduce the elastic behavior of the

film and avoid deformation of the material during the slicing with a fresh razor blade.

The liquid was pumped through the MCF using a M Series syringe-free liquid handling pump

(Valco Instruments Co. Inc. VICI AG International) capable of operating in the flow range of 5 nL·

min$^{-1}$ to 10 mL·min$^{-1}$. The RTD experiments required two pumps to flow the water and the tracer

aqueous solution.

The array photoreactor consisted of the MCF coiled around a tubular germicidal lamp (Germicidal

G8T5, GE Lighting, Northampton, UK) emitting radiation at 254 nm with a nominal power of 8 W

(Fig. 2). The lamp bulb was 302 mm long and with a diameter of 16 mm. The film was held in place

by two plastic pegs in the center section of the lamp in which light irradiance was found uniform.

The section of the MCF not coiled around the germicidal lamp was covered with aluminum foil to

prevent light irradiation. The residence time in the reactor and exposure to UV was varied by varying the length of MCF coiled over the lamp.

The lamp irradiance and therefore the incident flux in the capillaries was varied by changing the nominal power supplied to the lamp from 4.5 W to 8.0 W using a variable power supply unit. The reactor was operated in continuous mode until steady state was reached ($\cong$ 200 s, i.e. 3 to 5 times the mean hydraulic time). Samples were then collected at both outlet and inlet of the MCF photoreactor and rapidly analyzed. To avoid operation at excessive pressure drops, the solution was recirculated to achieve reaction times higher than the mean residence time in the MCF.

All the experimental runs were carried out at room temperature (20 °C), and the temperature of the fluids remained constant along the experiment (data not shown). The pH of the solutions was adjusted using diluted solutions of NaOH and $H_2SO_4$. At the end of each experimental run, the pH of the solutions was unchanged.

For RTD determination two pumps connected to an automatic multi-inlet valve was used to switch the inlet of the MCF from clean water to the Blue Dextran solution. Each experiment started by following water through the microreactor until a baseline was established in the UV detector (see section 2.3). The valve was then switched to the tracer solution producing a step change in concentration, and monitored until the outlet reached a stationary state (i.e., three to five times the mean residence time).

2.3. Analytical methods

The entire section of the MCF material was imaged real-time in UV for measuring the RTD tracer using an ActiPix™ D100 UV Area Imaging System microfluidic monitor (Paraytec, York, UK) equipped with a 214 nm dichronic filter. The viscosity of the tracer solution was determined using a AR1000-N (TA Instruments) rotational rheometer.

The concentrations of hydrogen peroxide, BE and caffeine in the samples were evaluated by HPLC (1100 Agilent) equipped with a Gemini C18 (Phenomenex) reverse phase column and a diode array

UV/VIS detector ($\lambda$ = 232 and 274 nm) and using a mobile phase flowing at 0.8 mL·min$^{-1}$. The mobile phase used for hydrogen peroxide and BE analyses consisted of a mixture of formic acid aqueous solution (25 mM) (A) and acetonitrile (B). The gradient used was as follows: 7% B to 28% B for 9 min, increased to 50% B in 5 min, constant for 2 min, and then decreased to 35.7% B in 3 min and, finally to 7% B in 5 min. The mobile phase for caffeine analysis consisted of formic acid aqueous solution (25 mM) (A) and methanol (C). In this case a linear gradient progressed from 5% C to 80% C in 14 min and then decreased to the initial conditions after 5 min. The initial and final pH of the solutions was measured with an Accumet Basic AB10 pH-meter. The molar absorption coefficients of caffeine and benzoylecgonine were estimated using a Perkin Elmer UV/VIS spectrometer (mod. Lambda 35).

3. Results and discussion

3.1. RTD determination

Rheological measurements were performed to determine the viscosity of the RTD tracer as a function of the shear rate. Figure 3 shows that the tracer solution viscosity remained very close to that of water and that was unaffected by shear rate. Varying the shear rate in the range 2-1000 s$^{-1}$, the ratio between the tracer and water viscosities remained close to 1.0.

The dynamic response of the normalized cumulative tracer concentration (empty circles) at the output of the MCF reactor for a step change at two different flow rates (0.6 mL·min$^{-1}$ and 1.0 mL·min$^{-1}$) is shown in Figures 4a–b respectively. The theoretical curve for an ideal Plug Flow Reactor (PFR, continuous line) and pure convective or Laminar Flow Reactor (LFR, dashed lines) are also shown.

Although the Reynolds number was well within the laminar flow regime (6.5 and 10.9 for flow rates of 0.6 mL·min$^{-1}$ and 1.0 mL·min$^{-1}$ respectively) the hydrodynamic behavior in the reactor approached that of an axially dispersed PFR, rather than a LFR. Similar observations have been

reported in other studies in microreactors [35-38] and it was in agreement with Taylor's theory on axial dispersion in reactors with a small $d/L$ ratio [39].

The MCF experimental data fitted well a Gaussian cumulative distribution function (CDF). The mean value and variance of the CDF distribution fitted well both the mean residence time and the axial dispersion in the reactor. The mean hydraulic time (39.7 s for 1.0 mL·min$^{-1}$ and 66.2 s for 0.6 mL·min$^{-1}$) matched closely the mean residence time determined from the experimental RTD data (40.5 s and 65.4 s, respectively), which also revealed the absence of dead volumes or sorption of the tracer on the microcapillaries walls [40].

The extent of axial dispersion in the MCF was estimated by fitting RTD data to a PFR with axial dispersion model, by finding the dimensionless dispersion number ($N_D$), which is given by the ratio of the axial dispersion ($D$) and the product of superficial velocity ($u$) and the reactor length ($L$):

$$N_D = \frac{D}{u \cdot L} \tag{1}$$

Depending on the magnitude of axial dispersion, one of the two following PFR with axial dispersion models was used [40]:

$$E = \sqrt{\frac{u^3}{4\pi DL}} \cdot exp\left[-\frac{(L-ut)^2}{\frac{4DL}{u}}\right] \qquad \text{(for } N_D < 0.01) \tag{2}$$

$$\left(\frac{\sigma}{\tau}\right)^2 = 2N_D - 2N_D^2 \cdot \left(1 - e^{-\frac{1}{N_D}}\right) \quad \text{(for } N_D > 0.01) \tag{3}$$

where $E$ and $\sigma$ represent the residence time distribution and the standard deviation respectively. Equation 2 can be easily reported as a function of $N_D$ and the ideal residence time $\tau$:

$$E = \sqrt{\frac{u^2}{4\pi L^2 N_D}} \cdot exp\left[-\frac{(L-ut)^2}{4L^2 N_D}\right] = \frac{1}{\tau}\sqrt{\frac{1}{4\pi N_D}} \cdot exp\left[-\frac{(t-\tau)^2}{4\tau^2 N_D}\right] \tag{4}$$

The $N_D$ values estimated from Equations 3 and 4 for the two flow rate conditions yielded very similar results (Table 1). Levenspiel reports that a tubular reactor can be successfully modeled as a PFR when $N_D$ is lower than 0.01 [40], however, other studies have shown that even for $N_D < 0.05$,

the PFR model yields very reliable results in term of conversion [38]. Therefore, the MCF photoreactor was considered an ideal PFR in the photolysis experiments.

3.2. Optical path length

Due to the absence of refractive phenomena [20], it can be assumed that the radiation emitted by the UV lamp is perpendicular to the surface of the bulb and crosses both the reactor and the reacting solution without any deviation of path length. Considering the circular section of the capillaries, the optical path length is determined by the intersection between the single UV ray and the capillary section.

As shown in Figure 5, there is only one ray on each capillary that crosses the section along the diameter length (chord *c-c'*). On the other hand, most of the UV rays cross the capillaries along a path shorter than the diameter (e.g. chords *a-a'* and *b-b'*). In consequence, the average diameter of the capillaries could not be taken as the average optical path length in the MCF. In contrast, the optical path length (*l*) of the capillaries was calculated as ratio between the mean hydraulic section (*S*) and the mean diameter of the capillaries (*d*) as follows:

$$l = \frac{S}{d} = \frac{\pi \cdot d^2}{4 \cdot d} = 152 \ \mu m \tag{5}$$

This operation corresponds to the mean integral value of the chords parallel to the incident radiation. Therefore, the cross section of a single capillary was considered to be equivalent to a rectangle (indicated in Figure 5 as equivalent section) oriented as shown in Figure 5 and with the same cross sectional area (*S*) as that of the circular capillary (indicated in Figure 5 as real section).

3.3. Estimation of lamp $UV_{254}$ photon flux

In order to better characterize the micro-photoreactor, the $UV_{254}$ photon flux ($q_{p,254}$) [41] incident on the reactor was first estimated. For microchannel reactors, this parameter is difficult to be directly estimated through radiometric measurements because of errors originating from measuring the flux from very small reactor surfaces and possible reflection phenomena from the surrounds.

8

Therefore, the photon flux was estimated from an indirect approach by determining the photolysis of an aqueous solution of hydrogen peroxide (reactions $r_1$ - $r_3$) at 254 nm [42] which was flowed through MCF.

$$H_2O_2 \xrightarrow{hv,\ \Phi_{254}^{H_2O_2}} 2\ HO° \qquad\qquad \Phi_{254}^{H_2O_2} = 0.55 \text{ mol·ein}^{-1} \quad [43] \qquad (r_1)$$

$$HO° +\ H_2O_2 \xrightarrow{k_h} HO_2° + H_2O \qquad\qquad k_h = 2.7·10^7 \text{ L·mol}^{-1}·\text{s}^{-1} \ [44] \qquad (r_2)$$

$$HO_2° + HO_2° \xrightarrow{k_t} H_2O_2 + O_2 \qquad\qquad k_t = 8.3·10^5 \text{ L·mol}^{-1}·\text{s}^{-1} \ [45] \qquad (r_3)$$

Considering the radical species ($HO_2°$ and $HO°$) at steady-state, the mass balance on hydrogen peroxide yielded:

$$\frac{d[H_2O_2]}{d\tau} = -2\frac{q_{p,254}}{V}·\Phi_{254}^{H_2O_2}·\left(1 - \exp\left(-2.3·l·\varepsilon_{254}^{H_2O_2}·[H_2O_2]\right)\right) \qquad (6)$$

where "$l$" is the optical pathlength of the micro-photoreactor, previously calculated (152 μm), "$\varepsilon_{254}^{H_2O_2}$" the molar absorption coefficient at 254 nm for hydrogen peroxide (18.6 L·mol$^{-1}$·cm$^{-1}$), $V$ the volume of reacting system (0.45 mL), "$\Phi_{254}^{H_2O_2}$" the primary quantum yield of the direct photolysis of hydrogen peroxide at 254 nm and $\tau$ the residence time. The photon flux "$q_{p,254}$" was estimated by an iterative method, which minimized the objective function $\sum_{i=1}^{n}(y_i - c_i)^2$, i.e., the squares of the differences between the calculated "$y$" and experimental "$c$" concentrations of hydrogen peroxide [46], where "$n$" is the number of experimental data collected during the photolysis of $H_2O_2$.

The ordinary differential equation (Eq. 6) was solved using MATLAB routine "ode45", which is based on the Runge-Kutta method with adaptive step-size. The numerical values for the UV$_{254}$

incident photon fluxes for two nominal lamp powers ($P_N$) and their uncertainties and percentage

standard deviations ($\sigma_\%$) are reported in Table 2.

The photolysis of hydrogen peroxide determined experimentally was compared to the values

predicted by the kinetic model, and this showed a goof fit (Figure 6).

In order to compare the nominal UV power ($P_N$) and the effective one, the latter has been expressed

in watts ($P^o_{254}$) using the following equation:

$$P^o_{254} = \frac{q_{p,254} \cdot h \cdot N_a \cdot c}{\lambda} \tag{7}$$

where "$h$" is Planck's constant ($6.63 \cdot 10^{-34}$ J·s), "$c$" the speed of light in vacuum ($3.0 \cdot 10^8$ m·s$^{-1}$),

"$N_a$" Avogadro's constant ($6.02 \cdot 10^{23}$) and "$\lambda$" the wavelength of the radiation emitted by the UV

lamp ($254 \cdot 10^{-9}$ m).


3.3. Model validation

The accuracy of the modeling methodology for the MCF was validated by estimating the quantum

yield of direct photolysis of caffeine at 254 nm ($\Phi^{CAF}_{254}$) in the MCF and determining its difference

from the quantum yield values reported in literature. Caffeine is often used as reference compound

since it is considered an anthropogenic marker of wastewater contamination in surface waters [47].

The quantum yield of caffeine, shown in Table 3, was calculated using the same optimization

procedure previously reported for the estimation of "$q_{p,254}$":

$$\frac{d[CAF]}{dt} = -\frac{q_{p,254}}{V} \cdot \Phi^{CAF}_{254} \cdot (1 - \exp(-2.3 \cdot l \cdot \varepsilon^{CAF}_{254} \cdot [CAF])) \tag{8}$$

where the term "$\varepsilon^{CAF}_{254}$" is the molar absorption coefficient at 254 nm for caffeine (4175 L·mol$^{-1}$·cm$^{-1}$). Literature data obtained using different photoreactor designs are also reported. Figure 7 shows

the UV$_{254}$ photodegradation of caffeine in the MCF as a function of the irradiation time and the

model prediction (equation 8) using the quantum yield values reported in Table 3. The model was

10

able to predict the photodegradation of caffeine with a good degree of confidence. The experimental results (full circles) were within the results of determined from equation 8 using the quantum yields from other studies (dashed line).

3.4. Direct photolysis of benzoylecgonine

The direct photolysis of BE under $UV_{254}$ irradiation was determined using the MCF photoreactor. Figure 8 shows that the rate of BE photolysis was not affected by pH in the range from pH 4.0 to 8.0. Additional control runs, carried out at pH 4.0, under dark conditions or with $UV_{254}$ irradiation but under an inert atmosphere (nitrogen bubbling), showed no difference in the photolysis of BE with respect to the data reported in Figure 8 (data not shown). This rules out the occurrence of hydrolytic mechanisms or photooxidative processes due to the presence of oxidant species such hydroxyl radicals or singlet oxygen than may be eventually produced under aerated conditions [50]. Following the same methodology reported for caffeine, the quantum yield of direct photolysis of BE ($\Phi_{254}^{BE}$) was estimated using simultaneously the data collected from two photolytic runs carried at pH 4.0 and 8.0 under irradiation with the $UV_{254}$ lamp with a nominal power of 8.0 W (*optimization mode*). Moreover, with the aim to validate the best estimate of $\Phi_{254}^{BE}$, the results of an additional photolytic run, carried out at pH 6.0 with the $UV_{254}$ lamp with a nominal power of 4.5 W, were modeled without any further adjustment of the $\Phi_{254}^{BE}$ parameter (*fitting mode*).

Table 4 shows the quantum yield for direct photolysis of BE $\Phi_{254}^{BE}$, the uncertainty percentage and standard deviations calculated on each experimental run.

The graphical comparison of the predicted and measured BE concentrations during the photolytic process is reported in Figure 9 for the set used in *optimization mode* and in Figure 10 for the data used in *fitting mode*. The analysis of the figures suggest a high degree of confidence of the proposed model to predict the photolytic decomposition of BE under the adopted experimental conditions.

4. Conclusions

A MCF array photoreactor made of fluoropolymer material was characterized by measuring the RTD. The flow regime was found to be approximately in the plug flow region at mean flow velocities below 1 mL·min$^{-1}$. The data of a first set of experimental runs on the MCF was used to predict the quantum yield of direct photolysis at 254 nm of caffeine (($7.48\pm0.64)\cdot10^{-4}$ mol·ein$^{-1}$) in unbuffered aqueous solutions.

The estimated value was located within the variability range previously identified by others through the results of measurements carried out in different conventional reactors.

Direct photolysis at 254 nm of benzoylecgonine was investigated in the pH range of 4.0 – 8.0. The consumption rates were not affected by the pH adopted. The photolysis quantum yield was $(6.22\pm0.19)\cdot10^{-3}$ mol·ein$^{-1}$.

The results collected demonstrate that the MCF photoreactor, adopted in the present investigation, is particularly useful for investigating the photochemical behavior of highly priced pharmaceuticals and illicit drugs and their human metabolites.

References

[1] W.Y Lin, Y. Wang, S. Wang, H.R. Tseng. Integrated microfluidic reactors. Nano Today 4 (2009) 470–481.

[2] P.L.Mills, D.J. Quiram, J.F. Ryley. Microreactor technology and process miniaturization for catalytic reactions–A perspective on recent developments and emerging technologies. Chem Eng. Sci. 62 (2007) 6992–7010.

[3] T. Wirth. Microreactors in Organic Chemistry and Catalysis, Ed. Wiley-VCH Verlag GmbH & Co. KGaA, Germany, 2013.

[4] Z. Nie, S. Xu, M. Seo, P.C. Lewis, E. Kumacheva. Polymer particles with various shapes and morphologies produced in continuous microfluidic reactors. J. Am. Chem. Soc. 127 (2005) 8058–8063.

[5] D.M. Roberge, L. Ducry, N. Bieler, P. Cretton, B. Zimmermann. Microreactor technology: A revolution for the fine chemical and pharmaceutical industries? Chem. Eng. Technol. 28 (2005) 318–323.

[6] F.R. Carrel, K. Geyer, J.D.C. Codee, P.H. Seeberger. Oligosaccharide synthesis in microreactors. Org. Lett. 9 (2007) 2285–2288.

[7] K. Geyer, P.H. Seeberger. Optimization of glycosylation reactions in a microreactor. Helv. Chim. Acta 90 (2007) 395–403.

[8] J. Pelleter, F. Renaud. Facile, fast and safe process development of nitration and bromination reactions using continuous flow reactors. Org. Process Res. Dev. 13 (2009) 698–705.

[9] H. Löwe, V. Hessel, A. Mueller. Microreactors. Prospects already achieved and possible misuse. Pure Appl. Chem. 74(12) (2002) 2271–2276.

[10] X. Zhang, S. Stefanick, F.J. Villani. Application of microreactor technology in process development. Org. Process Res. Dev 8 (2004) 455–460.

[11] B.P. Mason, K.E. Price, J.L. Steinbacher, A.R. Bogdan, D.T. McQuade. Greener approaches to organic synthesis using microreactor technology. Chem. Rev. 107 (2007) 2300–2318.

[12] E.M. Chan, A.P. Alivisatos, R.A. Mathies. High-temperature microfluidic synthesis of CdSe nanocrystals in nanoliter droplets. J. Am. Chem. Soc. 127(40) (2005) 13854–13861.

[13] R.M. Schoenherr, M.L. Ye, M. Vannatta, N.J. Dovichi, CE-microreactor-CE-MS/MS for protein analysis. Anal. Chem. 79 (2007) 2230–2238.

[14] R.A. Brennen, H. Yin, K.P. Killeen, Microfluidic gradient formation for nanoflow chip, Anal. Chem. 79(24) (2007) 9302–9309.

[15] M. Oelgemöller, O. Shvydkiv, Recent advances in microflow photochemistry. Molecules 16 (2011) 7522–7550.

[16] M. Oelgemöller, Highlights of photochemical reactions in microflow reactors, Chem. Eng. Technol. 35(7) (2012) 1144–1152.

[17] E.E. Coyle, M. Oelgemöller. Micro-photochemistry: photochemistry in microstructured reactors. The new photochemistry of the future? Photochem. Photobiol. Sci. 7 (2008) 1313–1322.

[18] S. Hejda, M. Drhova, J. Kristal, D. Buzek, P. Krystynik, P. Kluson, Microreactor as efficient tool for light induced oxidation reactions, Chem. Eng. J. 255 (2014) 178–184.

[19] S. Aida, K. Terao, Y. Nishiyama, K. Kakiuchi, M. Oelgemoller, Microflow photochemistry—a reactor comparison study using the photochemical synthesis of terebic acid as a model reaction, Tetrahedron Lett. 53 (2012) 5578–5581.

[20] N.M. Reis, G. Li Puma, Novel microfluidics approach for extremely fast and efficient photochemical transformations in fluoropolymer microcapillary films, Chem. Commun. 51 (2015) 8414–8417.

[21] M. Huerta-Fontela, M.T. Galceran, J. Martin, F. Ventura, Occurrence of psychoactive stimulatory drugs in wastewaters in north-eastern Spain, Sci. Total Environ. 397 (2008) 31–40.

[22] B. Kasprzyk-Hordern, R.M. Dinsdale, A.J. Guwy, The removal of pharmaceuticals, personal care products, endocrine disruptors and illicit drugs during wastewater treatment and its impact on the quality of receiving waters. Water Res. 43 (2009) 363–380.

[23] J.D. Berset, R. Brenneisen, C. Mathieu, Analysis of llicit and illicit drugs in waste, surface and lake water samples using large volume direct injection high performance liquid chromatography – Electrospray tandem mass spectrometry (HPLC–MS/MS), Chemosphere. 81 (2010) 859–866.

[24] A.L.N. Van Nuijs, B. Pecceu, L. Theunis, N. Dubois, C. Charlier, P.G. Jorens, L. Bervoets, R. Blust, H. Neels, A. Covaci. Cocaine and metabolites in waste and surface water across Belgium. Environ. Pollut. 157 (2009)123–129.

[25] E. Zuccato, S. Castiglioni, R. Bagnati, C. Chiabrando, P. Grassi, R. Fanelli, Illicit drugs, a novel group of environmental contaminants. Water Res. 42 (2008a) 961–968.

[26] E. Zuccato, C. Chiabrando, S. Castiglioni, R. Bagnati, R. Fanelli, Estimating community drug abuse by wastewater analysis. Environ. Health Perspect. 116 (2008b) 1027–1032.

[27] A.L.N. van Nuijs, S. Castiglioni, I. Tarcomnicu, C. Postigo, M.J. Lopez de Alda, H. Neels, E. Zuccato, D. Barcelo, A. Covaci, Illicit drug consumption estimations derived from wastewater analysis: a critical review, Sci. Total Environ. 409 (2011) 3564–3577.

[28] G. Orona, C. Campos, L. Gillerman, M. Salgot, Wastewater treatment, renovation and reuse for agricultural irrigation in small communities, Agr. Water Manage. 38(3) (1999) 223–234.

[29] D. Christova-Boal, R.E. Eden, S. McFarlane. An investigation into greywater reuse for urban residential properties. Desalination. 106(1–3) (1996) 391–397.

[30] A. Binelli, I. Marisa, M. Fedorova, R. Hoffmann, C. Riva, First evidence of protein profile alteration due to the main cocaine metabolite (benzoylecgonine) in a freshwater biological model, Aquat. Toxicol. 140–141 (2013) 268–278.

[31] M. Parolini, A. Binelli, Adverse effects induced by ecgonine methyl ester to the zebra mussel: A comparison with the benzoylecgonine, Environ. Pollut. 182 (2013b) 371–378.

[32] M. Parolini, A. Pedriali, C. Riva, A. Binelli, Sub-lethal effects caused by the cocaine metabolite benzoylecgonine to the freshwater mussel *Dreissena polymorpha*, Sci. Total Environ. 444 (2013a) 43–50.

[33] A.I. Barbosa, A.P. Castanheira, A.D. Edwards, N.M. Reis, A lab-in-a-briefcase for rapid prostate specific antigen (PSA) screening from whole blood,. Lab Chip. 14 (2014) 2918–2928.

[34] B. Hallmark, F. Gadala-Maria, M.R. Mackley, The melt processing of polymer microcapillary film (MCF), J. Non-Newtonian Fluid Mech. 128 (2005) 83–98.

[35] F. Trachsel, A. Günther, S. Khan, K.F. Jensen, Measurement of residence time distribution in microfluidic systems, Chem. Eng. Sci. 60 (2005) 5729–5737.

[36] C.H. Hornung, M.R. Mackley, The measurement and chatacterisation of residence time distributions for laminar liquid flow in plastic microcapillary arrays, Chem. Eng. Sci. 64 (2009) 3889–3902.

[37] C.H. Hornung, B. Hallmark, M. Baumann, I.R. Baxendale, S.V. Ley, P. Hester, P. Clayton, M.R. Mackley, Ind. Eng. Chem. Res. 49 (2010) 4576–4582.

[38] E. Georget, J.L. Sauvageat, A. Burbidge, A. Mathys, Residence time distributions in a modular micro reaction system, J. Food Eng. 116 (2013) 910-919.

[39] G. Taylor, Dispersion of soluble matter in solvent flowing slowly through a tube, Proc. R. Soc. A. 219 (1953) 186.

[40] O. Levenspiel, Chemical Reaction Engineering, third ed., John Wiley & Sons, New York, 1999.

[41] IUPAC. Compendium of Chemical Terminology, 2nd ed. (the "Gold Book"). Compiled by A. D. McNaught and A. Wilkinson. Blackwell Scientific Publications, Oxford (1997).

[42] I. Nicole, J. De Laat, M. Doré, J.P. Duguet, C. Bonnel, Use of UV radiation in water treatment: measurement of photonic flux by hydrogen peroxide actinometry, Water Res. 24 (1990) 157-168.

[43] S. Goldstein, D. Aschengrau, Y. Diamant, J. Rabani, Photolysis of aqueous $H_2O_2$: quantum yield and applications for polychromatic UV actinometry in photoreactors, Environ. Sci. Technol. 41 (2007) 7486–7490.

[44] G.V. Buxton, C.L. Greenstock, W.P. Helman, A.B. Ross, Critical review of rate constants for reactions of hydrated electrons, hydrogen atoms and hydroxyl radicals ($OH/O^-$) in aqueous solution, J. Phys. Chem. Ref. Data 17 (1988) 513–886.

[45] B.H. Bielski, D.E. Cabelli, R.L. Aruda, A.B. Ross, Reactivity of $HO_2/O_2$ radicals in aqueous solution, J. Phys. Chem. Ref. Data 14 (1985) 1041–1077.

[46] G.V. Reklaitis, A. Ravindran, K.M. Regsdell, Engineering Optimization, Wiley, New York, 1983.

[47] I.J. Buerge, T. Poigner, M.D. Müller, H.R. Buser. Caffeine, an anthropogenic marker for wastewater contamination of surface waters. Environ. Sci. Technol. 37 (2003) 691–700.

[48] Z. Shu, J. R. Bolton, M. Belosevic, M. G. El Din, Photodegradation of emerging micropollutants using the medium-pressure UV/$H_2O_2$ Advanced Oxidation Process, Water Res. 47 (2013) 2881-2889.

[49] J. Rivas, O. Gimeno, T. Borralho, J. Sagasti, UV-C and UV-C/peroxide elimination of selected pharmaceuticals in secondary effluents, Desalination. 279 (2011) 115–120.

[50] R. Marotta, D. Spasiano, I. Di Somma, R. Andreozzi. Photodegradation of naproxen and its photoproducts in aqueous solution at 254 nm: a kinetic investigation. Wat Res. 47 (2013) 373–383.

**Table**

| $Q$ (mL·min$^{-1}$) | 0.6 | 1.0 |
|---|---|---|
| Reynolds dimensionless number | 6.5 | 10.9 |
| **Theoretical residence** time, $\tau$ (s) | 39.7 | 66.2 |
| Experimental average residence time (s) | 40.5 | 65.4 |
| $N_D$ (estimated by Eq.**4**) | 0.0174 | 0.0223 |
| $N_D$ (estimated by Eq.**3**) | 0.0181 | 0.0229 |

Table 1

| $P_N$ (W) | $q_{p,254}$ ($ein \cdot s^{-1}$) | $\sigma_\%{}^{(*)}$ | $P^o_{254}$ (W) |
|---|---|---|---|
| 4.5 | $(5.71\pm0.20)\cdot10^{-6}$ | 0.68 | 2.69 |
| 8.0 | $(8.66\pm0.22)\cdot10^{-6}$ | 0.20 | 4.08 |

Table 2

| $\Phi_{254}^{CAF}$ (mol·ein$^{-1}$) | Present work | Shu et al., 2013[a] [48] | Rivas et al., 2011[b] [49] |
| --- | --- | --- | --- |
|  Caffeine | $(7.48\pm0.64)\cdot10^{-4}$ | $(3.0\pm1.0)\cdot10^{-4}$ | $(1.8\pm0.3)\cdot10^{-3}$ |
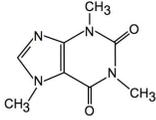
Table 3

| | $\Phi_{254}^{BE}$ (mol·ein$^{-1}$) | $\sigma_\%$ |
|---|---|---|
|  Benzoylecgonine $\varepsilon_{254}^{BE} = 1684$ L·mol$^{-1}$·cm$^{-1}$ | $(6.22\pm0.19)\cdot10^{-3}$ | *Optimization mode*<br>0.21 (pH 4.0, $P_N$ 8 W)<br>0.71 (pH 8.0, $P_N$ 8 W)<br><br>*Simulation mode*<br>0.36 (pH 6.0, $P_N$ 4.5 W) |

Table 4

**Figure**
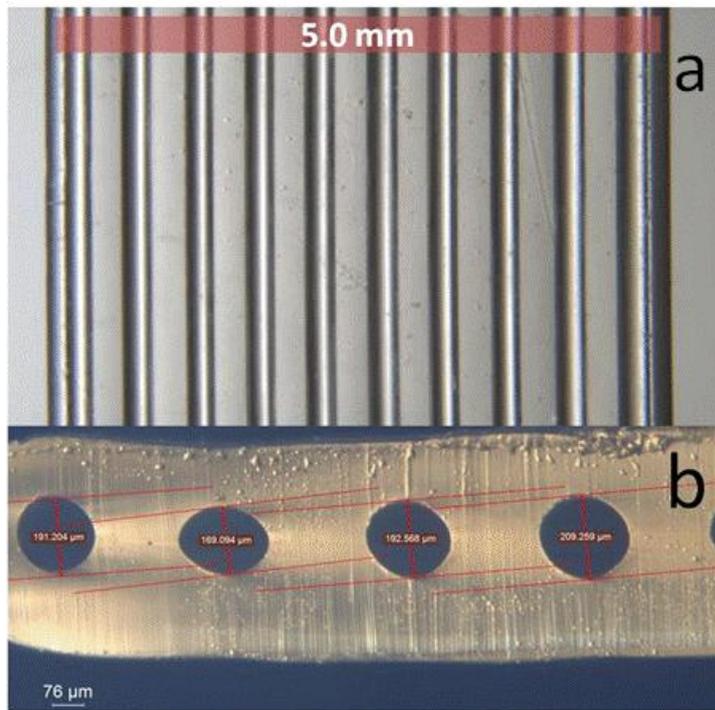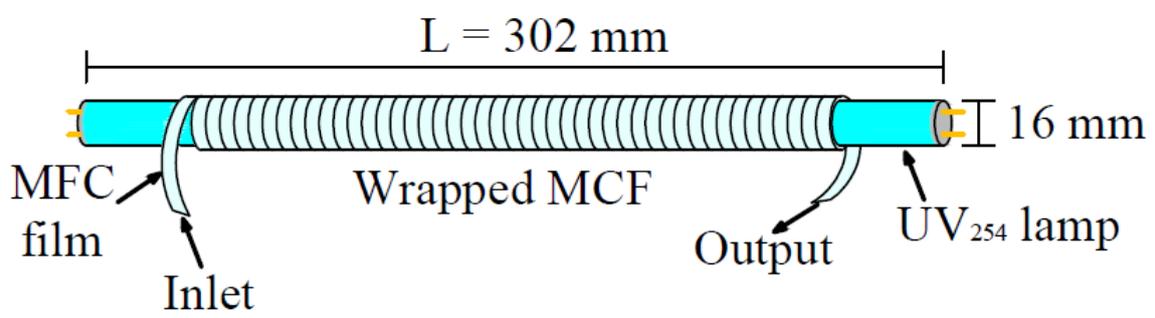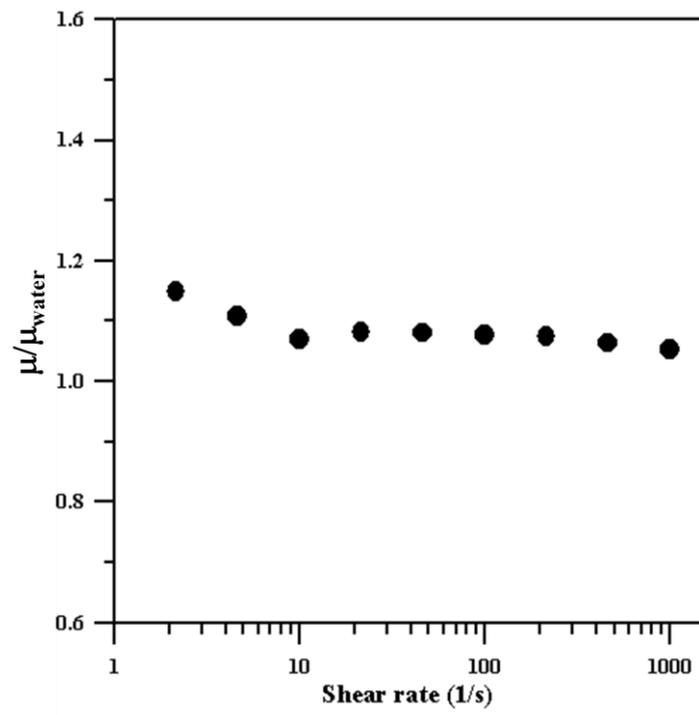


Fig. 1

Fig. 2

Fig. 3
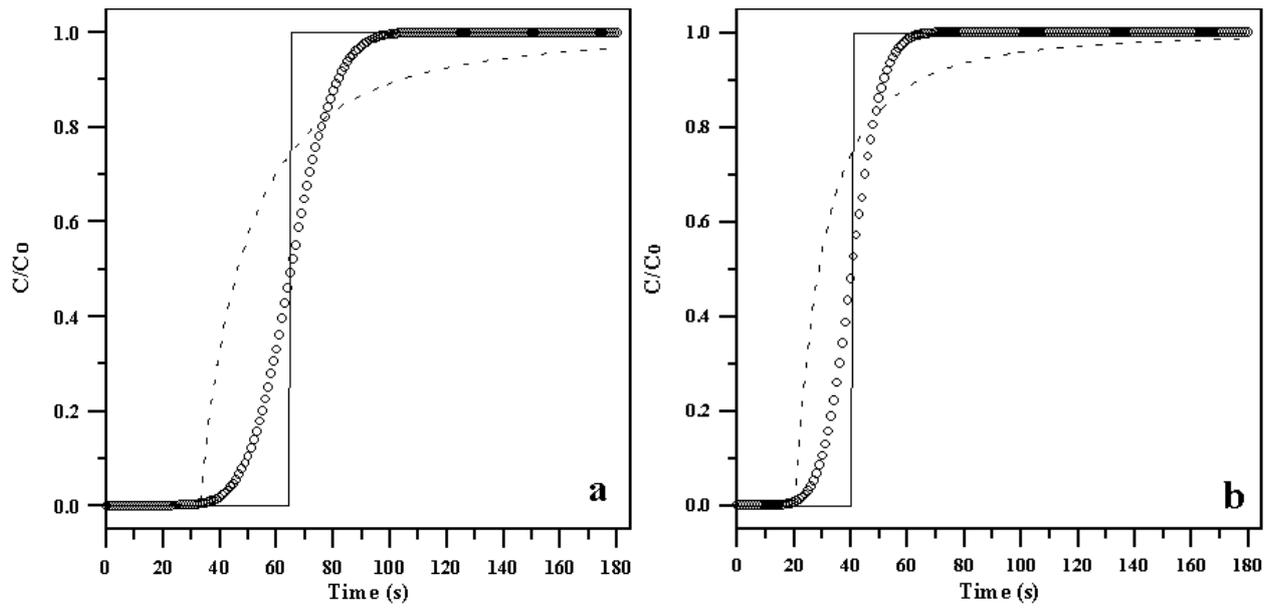
Fig. 4
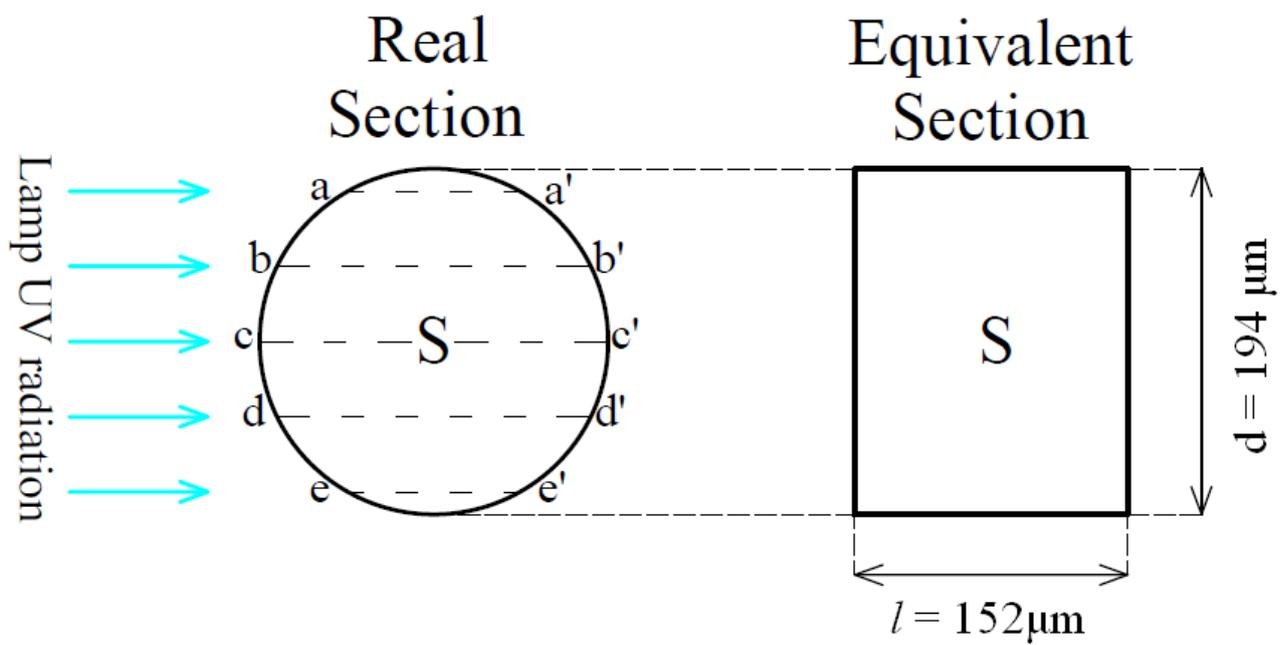
Fig. 5
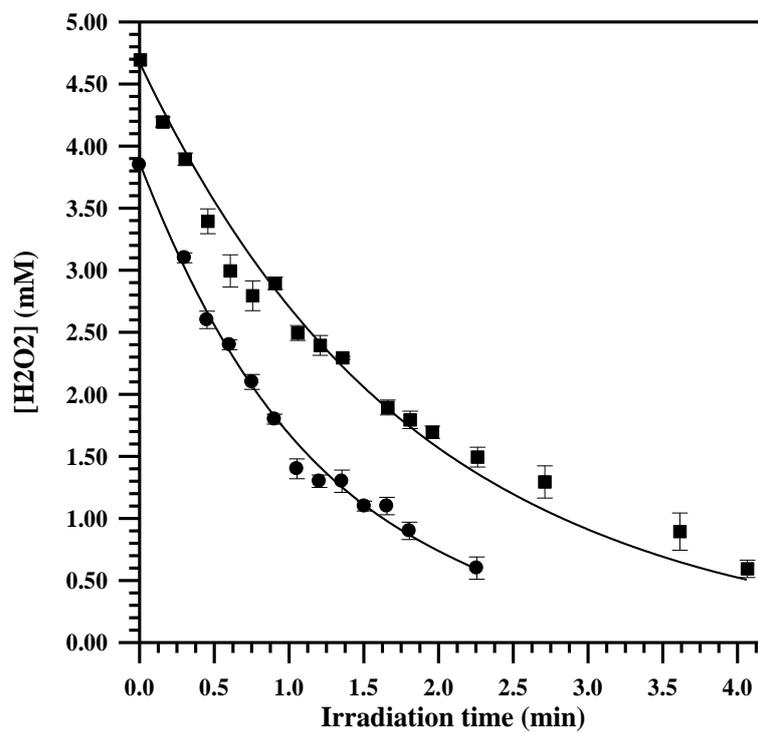
Fig. 6
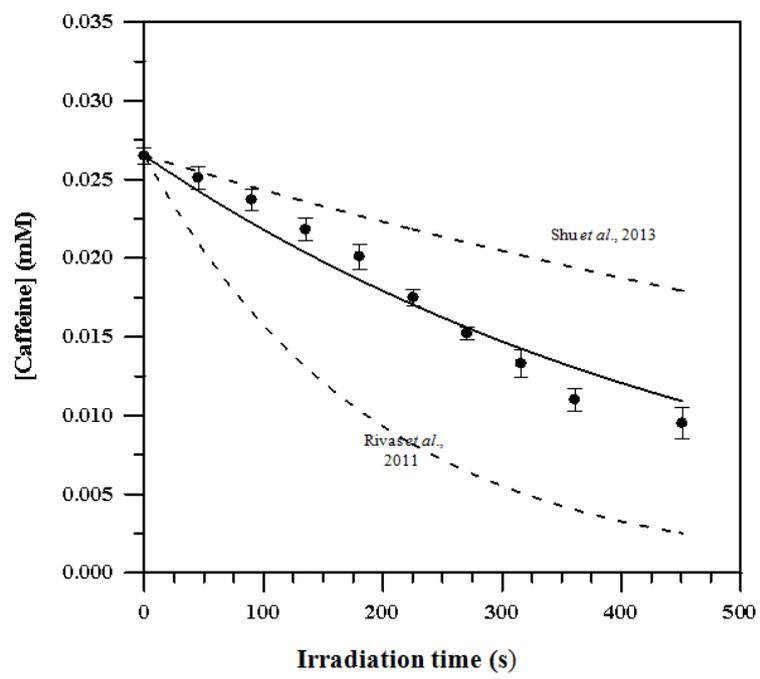
Fig. 7
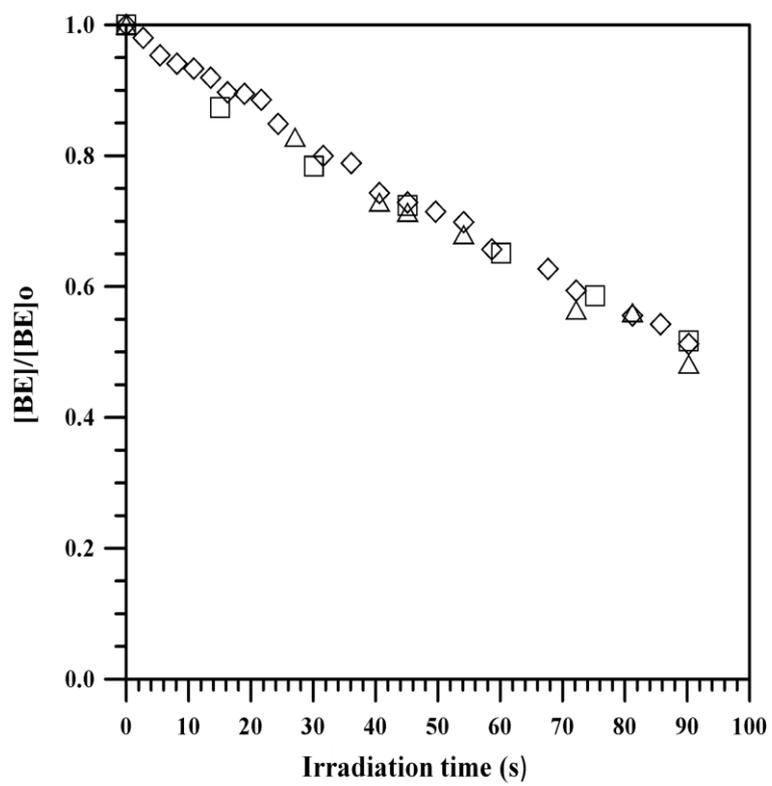
Fig. 8
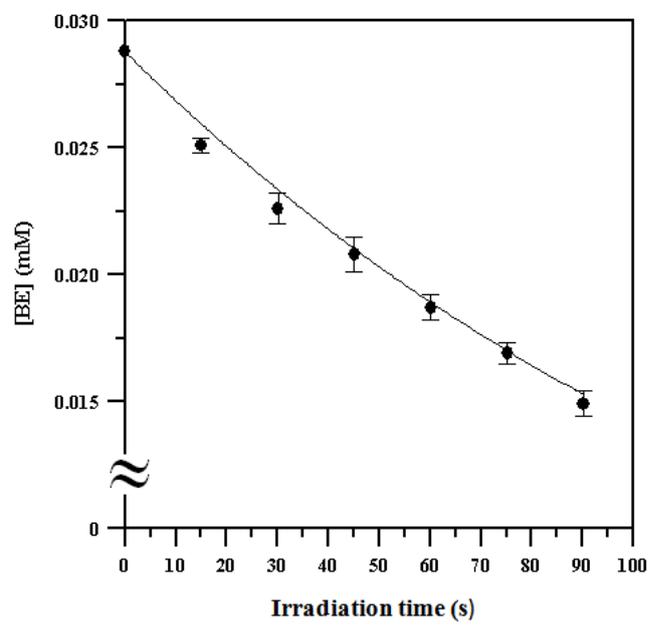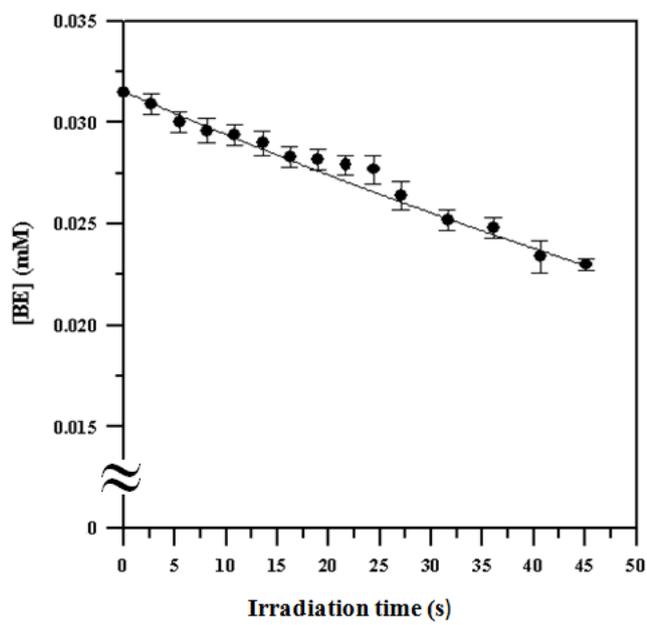
Fig. 9
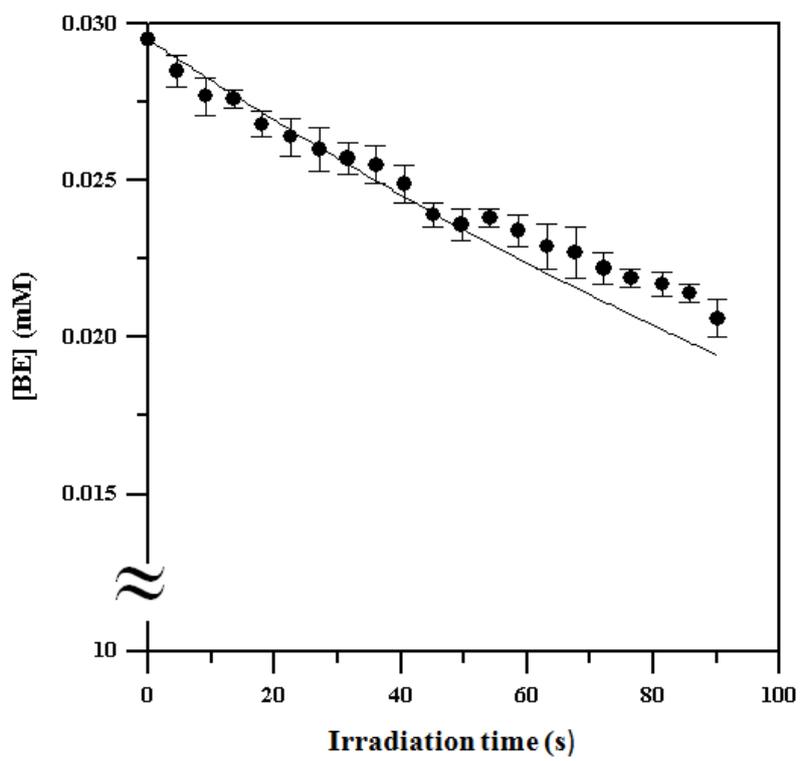
Fig. 10

Captions

Fig. 1: Details of microcapillaries acquired through the optical microscope: (**a**) structured plate with microchannels, (**b**) cross sections of the microchannels.

Fig. 2: Assembled MCF photochemical reactor (Loughborough University).

Fig. 3: Tracer relative viscosity at different shear rates.

Fig. 4: Experimental and theoretical normalized tracer concentrations during two experimental runs carried out with a flow rate of 0.6 mL·min$^{-1}$ (**a**) and 1.0 mL·min$^{-1}$ (**b**). (○) Experimental concentrations. (—) Plug Flow Reactor simulation. (- - -) Laminar Flow Reactor simulation.

Fig. 5: Reference simplified scheme for the average optical path length calculation.

Fig. 6: Predicted (solid lines) and experimental (symbols) concentration-time profiles for $H_2O_2$ $UV_{254}$–photolysis at different nominal lamp power. ● $P_N = 8.0$ W, $[H_2O_2]_o = 3.85$ mM; ■ $P_N = 4.5$ W, $[H_2O_2]_o = 4.70$ mM. pH $= 5.5 – 6.0$ and T $= 25$ °C.

Fig. 7: Predicted concentration profiles for photolysis of caffeine: present work data (solid line), literature (dashed line). Experimental data: full circle. pH $= 5.5 – 6.0$

Fig. 8: Direct photolysis of BE in bidistilled water at different pH using a $UV_{254}$ lamp with a nominal power of 8 W. ◇: pH 4.0, $[BE]_o$ $3.15 \cdot 10^{-2}$ mM; □: pH 6.0, $[BE]_o$ $2.88 \cdot 10^{-2}$ mM; △: pH 8.0, $[BE]_o$ $2.73 \cdot 10^{-2}$ mM.

Fig. 9: Calculated (solid line) and experimental (full circle) concentration profiles for $UV_{254}$-photolysis of BE at pH $= 4.0$ (left) and pH=8.0 (right) in *optimization mode*. Nominal lamp power: 8 W.

Fig. 10: Calculated (solid line) and experimental (full circle) concentration profiles for $UV_{254}$-photolysis of BE at pH $= 6.0$ in *simulation mode*. Nominal lamp power: 4.5 W.

Table 1: Calculated parameters for the continuous flow MCF photoreactor.

Table 2:  Best estimated values for $UV_{254}$ photon flux for different nominal powers of the UV lamp.

(*) $\sigma_{\%} = \frac{1}{\bar{c}} \cdot \sqrt{\frac{\sum_{i=1}^{n}(y_i - c_i)^2}{n-1}} \cdot 100$  where $\bar{c}$ indicates the average experimental concentration of $H_2O_2$.

Table 3: Quantum yields of caffeine  in the present work and reference values from literature including confidence intervals. [a] DI water, pH = 7.0; [b] Ultra Pure water, pH = 5.5 – 6.0.

Table 4: Best estimated value for $\Phi_{254}^{BE}$, confidence intervals and standard deviations.